JOURNAL OF THE PHYSICAL SOCIETY OF JAPAN, Vol. 48, No. 6, JUNE, 1980

X-Ray Structural Study of Ferroelectric Cesium Dihydrogen Phosphate at Room Temperature

Hironori MATSUNAGA, Kazuyuki ITOH
and Eiji NAKAMURA

Faculty of Science, Hiroshima University, Hiroshima 730

(Received January 14, 1980)

The atomic coordinates and the anisotropic thermal parameters of CsH_2PO_4 crystal in the paraelectric phase have been obtained using three-dimensional X-ray intensity data collected by a four-circle automatic diffractometer at room temperature. The structure is refined to $R=0.029$ for 780 independent reflections. Two types of hydrogen bonds are clearly distinguished in the electron density maps which display distributions corresponding to order and disorder of protons, respectively.

§1. Introduction

Cesium dihydrogen phosphate (abbreviated to CDP), CsH_2PO_4, exhibits ferroelectric activity below about $-120°C$.[1] Uesu and Kobayashi[2] determined the crystal structure at room temperature. They showed that CDP is monoclinic with the space group $P2_1/m$ in the paraelectric phase in contrast with many other KH_2PO_4-type ferroelectrics which belong to the tetragonal system in the paraelectric phase. The transition temperature of CDP is greatly dependent on deuteration[1] as in the case of KH_2PO_4-type ferroelectrics. The diffuse scattering study reveals the existence of one-dimensional ordering of the hydrogen bond parallel to the ferroelectric b-axis in CsD_2PO_4 which is isostructural with CDP.[3] Recently, Nelmes and Choudhary[4] have refined the structure by neutron diffraction study with the R-factor $R=0.049$, but they did not give thermal parameters. They have reported that one of the hydrogen bonds, which links phosphate groups parallel to the b-axis, is probably disordered by the R-factor ratio test.

It is worthwhile to investigate the structure of CDP in more detail to clarify the nature of the ferroelectric phase transition with one-dimensional correlation. In the present study an X-ray refinement of the structure at room temperature will be reported as a step to elucidate the mechanism of the phase transition of CDP in comparison with KH_2PO_4 from the structural point of view.

§2. Experimental

The compound CDP was prepared by the reaction

$$Cs_2CO_3+P_2O_5+2H_2O=2CsH_2PO_4+CO_2,$$

and single crystals were grown by slow evaporation from an aqueous solution at room temperature. The form of the specimen used in the present study was an elliptical cylinder with diameters $d_{max}\approx 0.10$ mm, $d_{min}\approx 0.06$ mm and hight $h\approx 0.10$ mm.

Bragg reflections were observed by a Rigaku automatic four-circle diffractometer controlled by PANAFACOM U100 computer, using MoKα radiation monochromatized by a graphite crystal and a scintillation counter connected to a pulse-height analyzer. The rotating anode tube was used for an X-ray source and the target loading was 50 kV × 170 mA. The unit cell parameters were determined by the least-squares method using 2θ values of 24 reflections. The results thus obtained are $a=7.912(2)$ Å, $b=6.383(1)$ Å, $c=4.8802(8)$ Å and $\beta=107.73(2)°$.

Integrated intensity data were collected with the ω-2θ scanning mode. The primary beam intensity was measured by a monitoring counter to make a correction for each Bragg intensity. The scanning speed was 8° per minute and the scan range $\Delta 2\theta$ was varied according to the relation $\Delta 2\theta=2.0°+0.8°\tan\theta$. The background intensities were measured for 2 seconds at the starting and end points of each scan. For the weak intensity reflections with $\sigma(|F_0|)>0.3|F_0|$

the measurements were repeated up to 4 times, where σ is the standard deviation estimated from counting statistics, and F_0 the observed structure factor. As a check of the stability of the crystal and the instruments, three standard reflections were monitored for every 200 reflections, but no significant variation of their intensities was noticed during the data-collection period. Independent 822 reflections corresponding to $\sin\theta/\lambda \leq 0.7\,\text{Å}^{-1}$ were measured and 780 of these, for which $|F_0| > 3\sigma(|F_0|)$, were used both for the least squares calculations and for the difference Fourier synthesis. The linear absorption coefficient of CDP is estimated as $\mu \approx 83.0\,\text{cm}^{-1}$ for MoKα radiation. However, as the absorption effect on the used reflections was negligibly small, no absorption correction was made.

§3. Refinement of the Structure

The results reported by Uesu and Kobayashi[2] were used as the starting parameters of the least squares calculation. Their isotropic thermal parameters were transformed to the anisotropic ones. The least squares calculations were made for the reflections with the same weight. At the final stage of the refinement all the atomic parameters were refined by means of the full matrix least squares calculations using 780 reflection data, of which 8 reflections were corrected for the extinction effect by Darwin's method. The calculation was converged with the final R-value of 0.029, where R is defined by $R=\sum||F_0|-|F_c||/\sum|F_0|$. Since the R-value was not improved by the correction of the anomalous dispersion effect, the final calculation was carried out without the correction of the anomalous dispersion effect. The atomic positions and the anisotropic thermal parameters, together with their estimated standard deviations (e.s.d's), are given in Table I. Assignment of the identification number to each atom was made in the same manner as Uesu and Kobayashi[2] as illustrated in Fig. 1. A three-dimensional difference Fourier synthesis was made using the final atomic parameters of non-hydrogen atoms. Figures 2(a) and (b) show the parts of the difference Fourier map around the hydrogen atoms H(1) and H(2), respectively. All the calculations were performed on a HITAC 8700 computer using the programs in UNICS.[5]

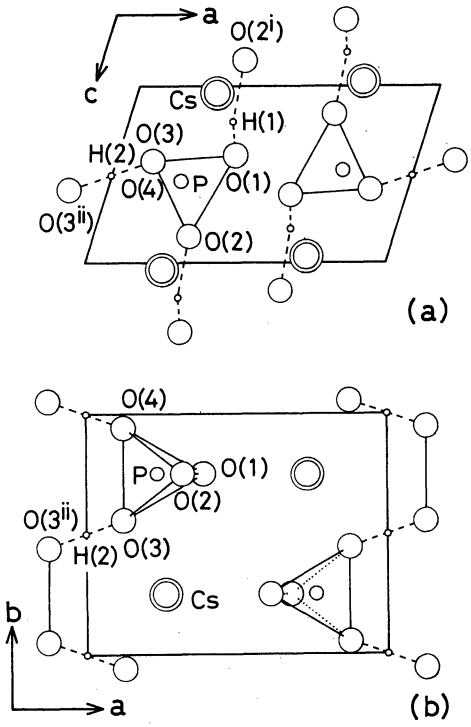

Fig. 1. Structure projected onto (a) (010) and (b) (001) planes.

Table I. Atomic fractional coordinates and thermal parameters U_{ij}, $U(\times 100)$ in Å^2 at room temperature, with their standard deviations in parentheses. The thermal parameters are defined by the formulae, $\exp[-2\pi^2(U_{11}h^2a^{*2}+U_{22}k^2b^{*2}+U_{33}l^2c^{*2}+2U_{12}hka^*b^*+2U_{13}hla^*c^*+2U_{23}klb^*c^*)]$ for U_{ij} and $\exp(-8\pi^2U\sin^2\theta/\lambda^2)$ for U.

	x	y	z	U_{11}, U	U_{22}	U_{33}	U_{12}	U_{13}	U_{23}
Cs	0.26569(6)	0.25	0.0354(1)	3.09(2)	2.60(2)	2.34(2)	0.0	0.64(2)	0.0
P	0.2370(2)	0.75	0.5293(3)	1.91(7)	2.41(8)	1.20(7)	0.0	0.75(6)	0.0
O(1)	0.3898(6)	0.75	0.3874(10)	2.1(2)	3.7(3)	1.5(2)	0.0	0.9(2)	0.0
O(2)	0.3222(5)	0.75	0.8447(11)	4.3(3)	6.1(4)	1.3(2)	0.0	1.3(2)	0.0
O(3)	0.1266(5)	0.5540(7)	0.4178(9)	4.3(2)	3.6(2)	4.2(2)	−1.2(2)	2.4(2)	−1.6(2)
H(1)	0.348(13)	0.75	0.195(24)	2.1(28)					
H(2)	0.0	0.5	0.5	5.5(41)					

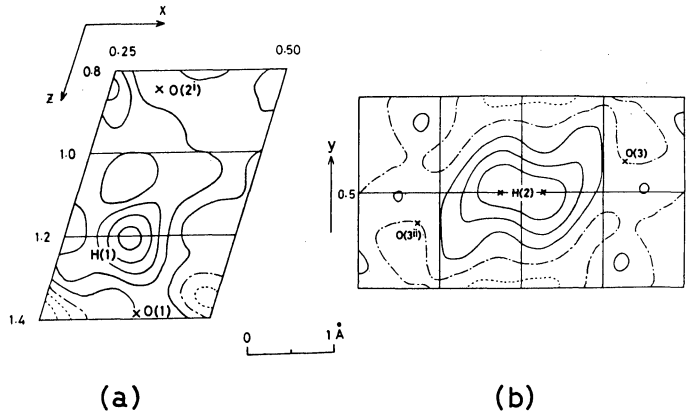

Fig. 2. The residual electron density around H(1) and H(2). The chain lines correspond to the zero density. The solid and dashed lines indicate positive and negative contours, respectively. The interval between the contours is 0.2 e/Å^3. (a) Section at $y=0.75$. (b) Section at the plane containing H(2) and O(3) atoms and parallel to the b-axis. The cross marks near H(2) indicate the two equilibrium positions of H(2) atom estimated by Nelmes and Choudhary.

§4. Results and Discussion

The atomic positions in Table I are almost consistent with the results reported by Nelmes and Choudhary,[4] but the e.s.d's of Cs and P atoms are less than theirs. The e.s.d's of H atoms are very large because the heavy atom such as Cs is contained in the crystal. Interatomic distances and bond angles, together with their e.s.d's, are shown in Table II. The root-mean-square displacements along the principal directions of thermal vibration for each atom are given in Table III.

Hydrogen bonds

The thermal parameter of H(2) atom is very large in comparison with that of H(1) atom as shown in Table I. The difference between two hydrogen atoms is also seen in the difference Fourier map (Figs. 2(a) and (b)). The distribution of the electron density of H(1) atom is found to be nearly isotropic, while that of H(2) atom is anisotropic and elongated on the plane at $y=0.5$. The cross marks around H(2) in Fig. 2(b) indicate the two equilibrium positions of H(2) atom estimated by Nelmes and Choudhary.[4] The contours for electron density of H(2) atom are consistent with their result. The bond distance of O(3)–H(2)$\cdots$O(3^{ii}) (2.47_2 Å) is shorter than O(1)–H(1)$\cdots$O(2^{i}) (2.53_7 Å) as can be seen in Table II. The former value is a little shorter than 2.49_6 Å in KH_2PO_4 and 2.51_9 Å in KD_2PO_4 at room temperature,[6] but longer than 2.40 Å which is the lower limit

Table II. Interatomic distances and bond angles of the phosphate group and hydrogen bonds at room temperature, with their standard deviations in parentheses.

Phosphate group			
P–O(1)	1.565(6) Å	O(1)–P–O(2)	107.0(3)°
P–O(2)	1.481(5)	O(1)–P–O(3)	106.1(2)
P–O(3)	1.529(4)	O(1)–P–O(4)	106.1(2)
P–O(4)	1.529(4)	O(2)–P–O(3)	113.6(2)
		O(2)–P–O(4)	113.6(2)
		O(3)–P–O(4)	109.9(2)
Hydrogen bond			
O(1)–O(2^{i})	2.537(7) Å	O(1)–H(1)–O(2^{i})	166(11)°
O(1)–H(1)	0.9(1)		
H(1)$\cdots$O(2^{i})	1.7(1)		
O(3)–O(3^{ii})	2.472(7)		

Table III. Parameters characterizing the principal directions 1, 2, 3 of thermal vibration for each atom: root-mean-square displacements (r.m.s.) and angles of the principal directions from a (ϕ_a), b (ϕ_b) and c (ϕ_c) axes.

		r.m.s.	ϕ_a	ϕ_b	ϕ_c
Cs	1	0.18 Å	5°	90°	113°
	2	0.16	90	0	90
	3	0.15	85	90	23
P	1	0.16	90	0	90
	2	0.14	152	90	101
	3	0.10	118	90	11
O(1)	1	0.19	90	0	90
	2	0.15	143	90	110
	3	0.11	53	90	160
O(2)	1	0.25	90	0	90
	2	0.21	162	90	90
	3	0.10	108	90	0
O(3)	1	0.25	63	124	58
	2	0.17	150	116	62
	3	0.15	101	45	45
H(1)		0.14			
H(2)		0.23			

of the length of the hydrogen bond with double minimum potential.[7]

Phosphate group

As shown in Table II, the PO_4 group is slightly deformed from a regular tetrahedron. Such a deformation is also found in other KH_2PO_4 family. The thermal vibrations of oxygen atoms in the PO_4 group are very anisotropic. Their longest principal axes of the thermal vibrtion ellipsoid are perpendicular to the directions of corresponding P–O bonds (Table III). The small root-mean-square displacements of the oxygen atoms are obtained in the directions of the corresponding P-O bond such as 0.12 Å for O(1), 0.13 Å for O(2) and 0.16 Å for O(3), respectively. Therefore, it should be considered that the phosphate group is in a librational motion. The anisotropic rigid-body translational and rotational vibration tensors were calculated for the PO_4 group from the thermal parameters of individual atoms on the basis of the model of Cruickshank.[8] It is found that the translational motion of the PO_4 group in the direction parallel to the c-axis is constrained and the rotational motion around the axis which lies in the ac-plane and forms 129° with the c-axis is about two times as large as those perpendicular to this axis. This direction is nearly parallel to the projection of H(2) bond on the ac-plane.

On the ferroelectric effect

In the ferroelectric phase, spontaneous polarization of CDP occurs along the b-axis. The H(2) hydrogen bonds link PO_4 groups together in the direction of the ferroelectric b-axis. As Fig. 2(a) shows H(2) atoms seem to be in a disordered state in the paraelectric phase. This suggests that ordering of H(2) atoms cause the spontaneous polarization through deformation of PO_4 tetrahedra as in the case of KH_2PO_4. As the H(1) atom is already in an ordered state at room temperature, the ordering of the hydrogen bond network in the ferroelectric phase is expected to occur only one-dimensionally. On the contrary, in KH_2PO_4 all the hydrogen bonds seem to be disordered in the paraelectric phase,[9] so that the ordering of the hydrogen bond develops in the three-dimensional hydrogen bond network. These results reflect the fact that the dielectric anomaly of CDP is only observed along the b-axis,[2] whereas in KH_2PO_4 it is also observed along the non-ferroelectric axes. These facts are consistent with that the diffuse scattering observed in CsD_2PO_4 is characterized by one-dimensional correlation, whereas that of KD_2PO_4 exhibits characteristics of correlations in a three-dimensional system.[3] To throw light on the mechanism of the ferroelectric phase transition in CDP, accurate structure analyses at several temperatures of both paraelectric and ferroelectric phases are in progress.

The authors are indebted to the Hiroshima University Computing Center for making the HITAC 8700 computer available to them.

References

1) A. Levstik, R. Blinc, P. Kadaba, S. Čižikov, I. Levstik and C. Filipič: Solid State Commun. **16** (1975) 1339.
2) Y. Uesu and J. Kobayashi: Phys. Status Solidi a **34** (1976) 475.
3) B. C. Frazer, D. Semmingsen, W. D. Ellenson and G. Shirane: Phys. Rev. B**20** (1979) 2745.
4) R. J. Nelmes and R. N. P. Choudhary: Solid State Commun. **26** (1978) 823.
5) *Universal Crystallographic Computing System*, ed. T. Sakurai (Japanese Crystallographic Association, 1967).
6) J. Nakano, Y. Shiozaki and E. Nakamura: J. Phys. Soc. Jpn. **34** (1973) 1423.
7) C. A. Coulson: *Valence* (Oxford, London, 1961) 2nd ed., p. 349.
8) D. W. J. Cruickshank: Acta Crystallogr. **9** (1956) 754.
9) R. J. Nelmes and K. D. Rouse: Ferroelectrics **8** (1974) 487.